

## **Direct Metal Laser Re-Melting (DMLR) of 316L Stainless Steel Powder**

### **Part 1: Analysis of Thin Wall Structures**

*Rhys Morgan, Adam Papworth, Chris Sutcliffe, Pete Fox, Bill O'Neill*  
*Research in Advanced Technologies Group*  
*Faculty of Engineering, The University of Liverpool, UK.*

#### **Abstract**

Direct Metal Laser Re-Melting is a process variant of Selective Laser Sintering, whereby 316L stainless steel powder fractions are melted by a high power Nd:YAG laser. Layers are built up as a series of single lines to produce thin walled structures in the range  $\approx 0.3-1.0$ mm thick. The structures exhibit a periodic, angular roughness to the wall surfaces. The samples also display a wave-like pattern on their upper surfaces. Further investigations reveal the angled 'wave' pattern exists on a macroscopic level in the microstructure. The pattern is fully formed by the third or fourth layer. Fern-like grain structures follow the orientation of the surface roughness and exist across many layers. This is believed to be the effect of grain orientation within the samples. The microstructure reveals long, needle, cell structures. The uni-axial needles grow epitaxially from previous layers. The samples have been shown to exhibit very little or no thermally induced residual stresses.

#### **Introduction**

Selective Laser Sintering has three main production routes for the processing of metallic components. The first two, Indirect Metal Sintering and Binary Phase Sintering involve, at some stage in the process, the use of alloy materials with properties poorer than that of the high strength, high temperature material in order to increase density or to improve melting and wetting characteristics (Tobin 1993; Bunnell, 1994). The parts produced, however, will not reproduce the exact materials characteristics of a similarly machined component.

The third route utilises only a single phase powder of the engineering material required for the fabricated end component. In this process, a high power laser beam directly melts and fuses the high temperature powder particles. There are, however, very significant problems associated with direct illumination of engineering alloys in this way. Firstly, large thermal gradients exist in the layers due to the non-homogenous heating of the powder by the laser. This causes substantial thermal stresses to be generated in the parts (Deckard, 1995). In polymer sintering processes, increasing bulk powder bed temperature reduces these thermal gradients. However, due to the high temperatures involved with direct laser sintering, anchor plates have been used to overcome

the effect of thermal stresses in the lasersintered part, and can be incorporated into the geometry of the final component (Meiners, 1998).

Final part density is a significant barrier to the success of single phase direct laser sintering. The molten volume is shaped through surface energy minimisation, driven by surface tension. There is also a possible effect of free convective “Marangoni” forces, as experienced in melt pools during laser welding (Lampa, 1997). These effects act to shape the volume into strings of connected melt beads, which are inherently difficult to tessellate and therefore create areas of porosity. Also, surface tension forces act to drag surrounding particles into the melt, causing local depleted areas of material (Song, 1997). Furthermore, high temperature oxidation of the material reduces wetting at the interface between layers and causes a greater degree of balling. These factors must be overcome for the successful production of fully dense, engineering alloy components for heavy duty, functional use. Research at the University of Liverpool is investigating Direct Metal Laser Remelting (DMLR) of stainless steel with Nd:YAG laser to achieve this goal.

#### **DMLR Experimental Arrangement**

The DMLR test facility consists of a Rofin Sinar 90W flash Q-Switched, Flash Lamp Pumped Nd:YAG Industrial Laser Marker and an atmospheric control chamber built in-house at the University of Liverpool. The Q-Switch of the Laser Marker facilitates pulsing of the output beam, with Pulse Repetition Frequencies (PRF) in the range 0 – 60kHz, where 0kHz is a Continuous Wave Output (CW). The Nd:YAG laser is preferred over CO<sub>2</sub> output beam, due to the improved coupling with the 1.064μm wavelength compared with 10.64μm, and hence greater absorption with metals (Tolochko, 2000); This reduces the input energy requirement and hence induces less thermally distortive effects. The integrated scanning mirrors enable a maximum scanning speed of up to 500mms<sup>-1</sup> over an 80x80mm square area. Minimum beam diameter at the focal length is measured as approximately 100μm.

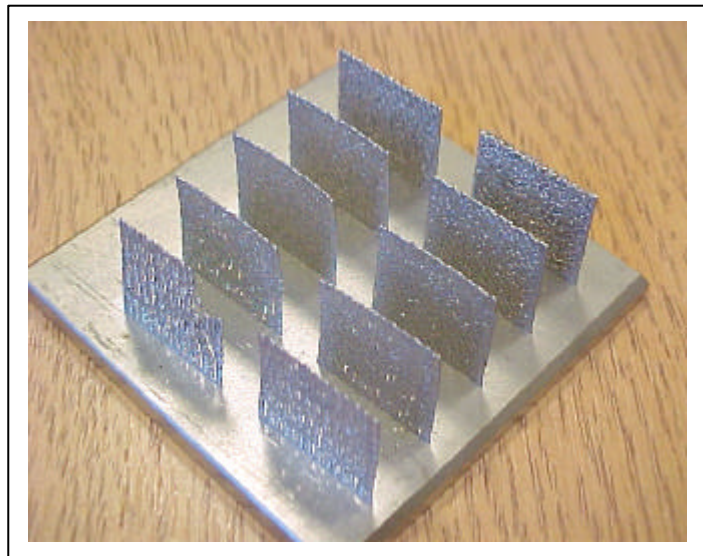


*Figure 1: Array of thin wall structures produced at varying scan speeds*

The Atmospheric Control Chamber is of typical SLS process chambers. It has a single powder feed cylinder with counter rotating roller mechanism for powder deposition onto the build platform. Layer thickness is controlled by stepper motors, whose minimum linear step size is  $1\mu\text{m}$ . The process is controlled by in-house software for full automation and communication between the system and laser marker. The system is enclosed to allow for evacuation of ambient environment and re-fill with Nitrogen process gas. No heaters are used before or during the process.

The material under investigation is Stainless Steel 316L. The powder is gas atomised (spherical), specified as  $80\% < 22\mu\text{m}$ , with a distribution approximately  $< 1\mu\text{m} < \phi < 60\mu\text{m}$ . It has the composition: 16.73Cr, 13.19Ni, 0.017C, 0.710Si, 2.69Mo, 1.6Mn, Fe balance (%wt).

Samples were ground and polished to  $1\mu\text{m}$ , and etched with standard austenitic (40% HCl, 20% HNO<sub>3</sub>, balance H<sub>2</sub>O) etch. A further "coloured" etch was employed to establish variations in composition within the austenite (4% Ammonium Hydrogen Difluoride, 16% Potassium Metabisulfite, balance H<sub>2</sub>O). This etchant highlights microstructures, which are chromium rich in blue, while nickel rich regions are shown in brown.

### Experimental Study

Initial experiments were undertaken to assess the effect of laser and scanning variables on cold, loose powder beds of arbitrary depth. Detailed results can be seen elsewhere (Morgan, 2001). A significant effect of scanning on loose powder layers, was the significantly increased beam absorption during the first scan lines, leading to increased volume of the coalesced melt beads, previously recognised as First Line Scan Balling (Hauser, 1999). The increased volume of these first scan lines causes problems when applying further powder layers. In order to overcome this effect, multiple layer experiments are undertaken on 3mm substrate plates of the same material.

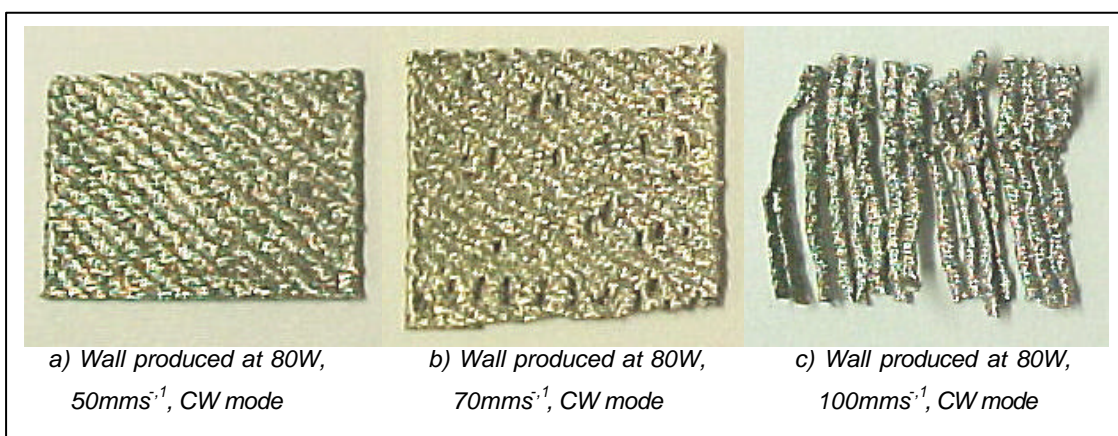


Figure 2: Thin Wall Structures Produced at Varying Scan Speeds

Ten single scan-line walls, of length 15mm, were produced per plate. The layer thickness was a constant 100 $\mu\text{m}$ . A hundred layers were produced during each experimental run. Due to the increased conduction effects from the substrate, power was kept at a maximum to ensure sufficient fusion between the powder layer and the plate. Average power was measured at 80W. Scan Speeds were varied in the range 10-500 $\text{mms}^{-1}$ . For this study, the samples were produced using CW mode scanning. The beam was set at the focal position, with a diameter of 100 $\mu\text{m}$ .

### Results and Discussion

Figure 1 shows a typical plate with thin wall structures. Each wall is produced with a different scan speed, incremented by 10 $\text{mms}^{-1}$ . Walls produced in the range 10-60 $\text{mms}^{-1}$  exhibit full density, with a diagonal pattern emerging in the surface as shown in Figure 2a. A threshold speed of 70 $\text{mms}^{-1}$  creates a step in the diagonal pattern resulting in areas of porosity within the structures (Figure 2b). Above 90 $\text{mms}^{-1}$ , the walls become a series of weakly connected vertical branches; the thickness of each branch reducing with increasing scan speed (Figure 2c). At scan speeds above 140 $\text{mms}^{-1}$ , there is insufficient energy imparted to the powder to affect bonding with the underlying layer, resulting in failure of the build. The thickness of the samples varies with scan speed. Increased thickness at the lower scan speeds is attributed to increased energy incident on the powder layer, resulting in radial conduction to the local surrounding powder, causing an increase in lateral melt volume and hence thicker walls. Also, there is a tendency for wall thickness to increase slightly with build height. This is due to the decreasing conduction

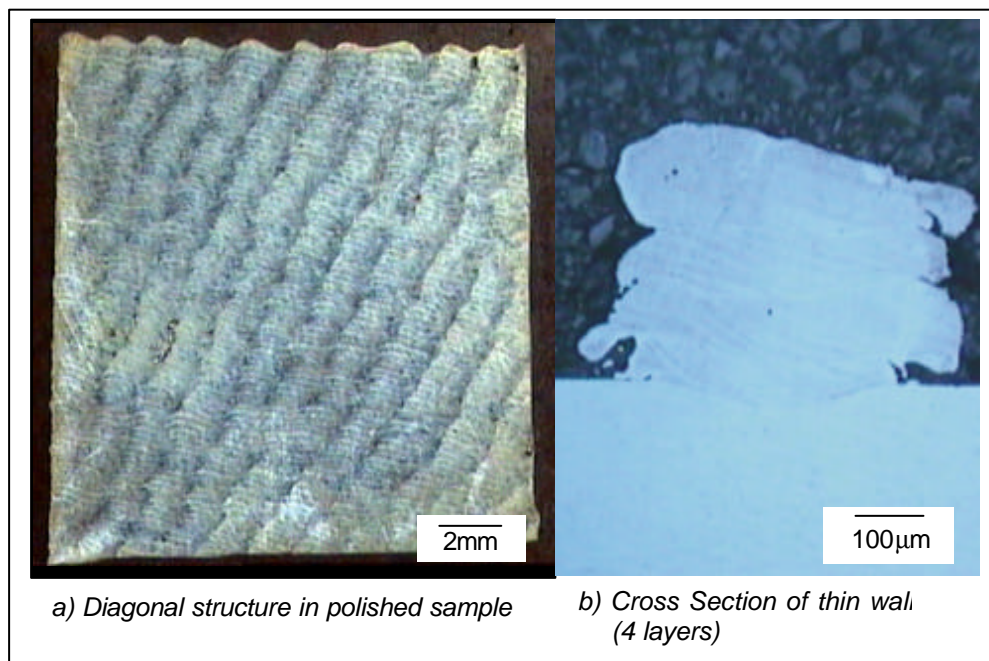


Figure 3: Formation of wave pattern in thin wall structures

effect from the substrate with increasing build height. The samples show no sign of deformation or residual stress; this was borne out when samples were annealed at 500°C for 4 hours and retained their form.

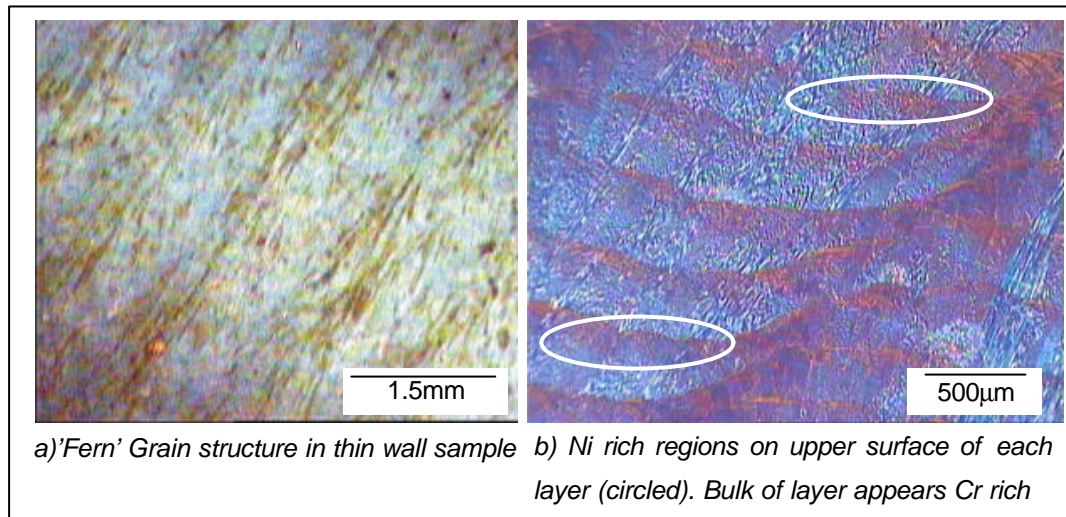


Figure 4: Analysis of microstructure with colour etch

Macroscopic analysis of the polished samples reveals the pattern on a macro-scale within the microstructure, while the upper surface of the samples exhibit a wave-like form (Figure 3a). The wave pattern has a periodicity of approximately 1.5mm. The wave structure evolves from the second or third layer; by the fourth layer it is fully established. A cross sectional view of the first three layers shows that a possible cause of the structure is due to the melt volume falling over the side of the wall (Figure 3b).

On closer examination of the polished samples, fern-like structures exist running along the diagonal pattern. These structures were initially thought to be the formation of nitrides. However, thermodynamically, this is not likely, as it is doubtful that there will be sufficient energy, in the time available, to disassociate the nitrogen to form a nitride. Also, replacing the Nitrogen process gas with Argon yielded the same grain structures. Using the colouring etch, the fern structures appear brown surrounded by light blue regions, suggesting regions of nickel rich grains (Figure 4a). However, it is more likely that the ferns are due to grain orientation within the microstructure. Further analysis of the samples with the colouring etch reveals the upper surface of each scan line is rich in nickel compared with the chromium rich bulk material of each layer (Figure 4b). This may be due to the differences in freezing temperatures between the chrome and nickel rich grain.

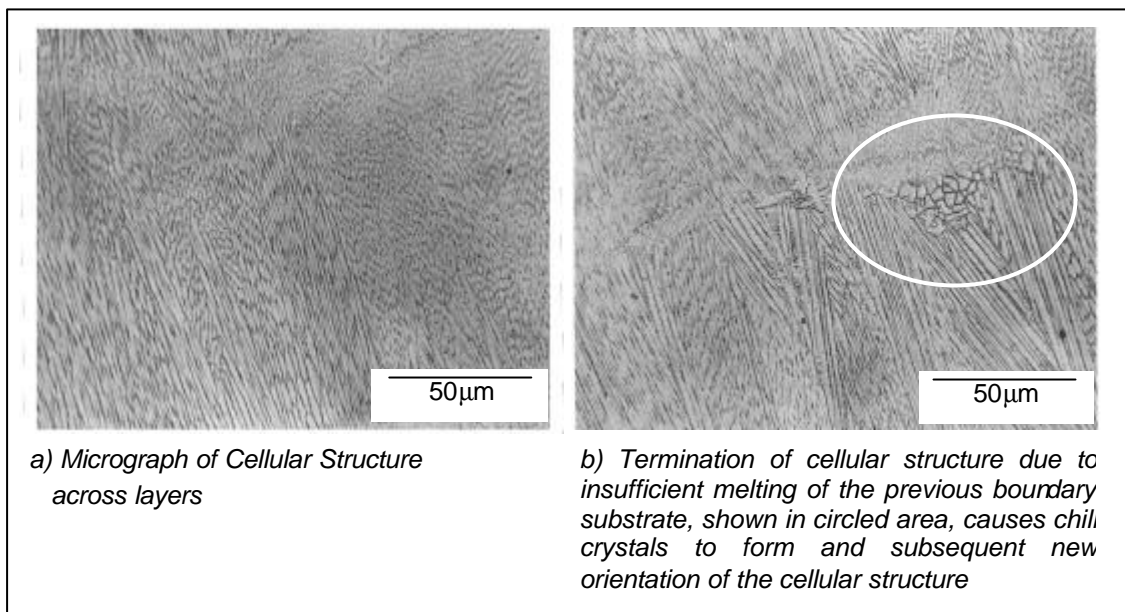


Figure 5: Microstructure of Direct Metal Laser Remelted Thin Wall Structures

High magnification microstructural analysis reveals, long needle shaped grains. These grains are due to the rapid solidification, where the formation of dendrite branching is restricted, resulting in a cellular structure (Figure 5a). Upon the passing of the beam, the underlying substrate (previous layer) is re-melted, causing the cellular structure to exhibit uni-axial, epitaxial growth. The columnar growth will continue throughout subsequent layers unless terminated by insufficient melting of the boundary substrate (previous layer) as marked in Figure 5b.

### Conclusions

The Direct Laser Re-Melting process has shown to produce full density thin walls (<1mm) at scan speeds < 70mms<sup>-1</sup>. The thin walls exhibit a wave-like pattern visible in the microstructure. This pattern is believed to be due to melt dynamics. Within the wave pattern, there appears a fern-like grain structure. This is believed to be due to grain orientation. The microstructure has shown full melting of the powder layers with no occurrence of unmelted particles. Grains exist along many layers, confirming melt metallurgic bonding between layers. Surprisingly, there appear to be no residual stresses in the walls. Scanning Transmission Electron Microscopy analysis is currently being undertaken to further assess the material structure.

### References

Tobin, J.R., Badrinarayan, B., Barlow, J.W., Beaman, J.J., Bourell, D.L., Indirect Metal Composite Part manufacture using the SLS process. Solid Freeform Fabrication Symposium. The University of Texas at Austin, Texas. Vol 4. 1993.

**Bunnell, D.E., Bourell, D.L., Marcus, H.L.,** Fundamentals of Liquid Phase Sintering Related to Selective Laser Sintering. Solid Freeform Fabrication Symposium, The University of Texas at Austin, Texas. 1994 pp. 379-385.

**Deckard, C., Miller, D.,** Improved Energy Delivery for Selective Laser Sintering  
Proc Solid Freeform Fabrication Symposium. The University of Texas at Austin, Texas. Vol. 6. 1995 pp. 151 - 158.

**Meiners, W., Wissenbach, K., Poprawe, R.,** Direct Generation of Metal Parts by Selective Laser Powder Remelting (SLPR). Proceedings of the International Congress on Applications of Lasers & Electro-Optics (ICALEO) 1998. Section E. pp. 31-36.

**Lampa, C., Kaplan, A. F. H., Powell, J., Magnusson, C.,** Analytical thermodynamic model of laser welding  
Journal of Physics D: Applied Physics, Vol. 30, No 9, (May 7 1997), pp. 1293-1299.

**Song, Y.A.,** Experimental study of the basic process mechanism for direct selective laser sintering of low-melting metallic powder. CIRP annals– Manufacturing Technology. 1997 46(1) pp. 127-130.

**Tolochko, N. K., Laoui, T., Khlopkov, Y. V., Mozzharov, S.E., Titov, V. I., Ignatiev, M. B.,** Absorbance of powder materials suitable for laser sintering. Rapid Prototyping Journal. Vol. 6, No 3, 2000 pp. 155-160.

**Morgan, R., Sutcliffe, C.J., O'Neill, W.,** Experimental Investigation of nanosecond pulsed Nd:YAG laser Re-Melted Pre Placed Powder Beds. Rapid Prototyping Journal. Vol. 7, No 3, 2001.

**Hauser, C., Childs, T.H.C., Dalgarno, K.W.** (1999, b) "Selective Laser Sintering of Stainless Steel 314S HC Processed Using Room Temperature Powder Beds", Proc Solid Freeform Fabrication Symposium, The University of Texas at Austin, Texas. Vol. 10, pp. 273-280.